Nuclear Inst. and Methods in Physics Research, A 953 (2020) 163141

Contents lists available at ScienceDirect

Nuclear Inst. and Methods in Physics Research, A

journal homepage: www.elsevier.com/locate/nima

A Study of NaI(Tl) crystal encapsulation using organic scintillators for the dark matter search

J.Y. Lee [a], G. Adhikari [b], C. Ha [c,*], H.J. Kim [a], N.Y. Kim [c], S.K. Kim [d], Y.D. Kim [b,c], H.S. Lee [c]

[a] Department of Physics, Kyungpook National University, Daegu 41566, Republic of Korea
[b] Department of Physics, Sejong University, Seoul 05006, Republic of Korea
[c] Center for Underground Physics, Institute for Basic Science (IBS), Daejeon 34126, Republic of Korea
[d] Department of Physics and Astronomy, Seoul National University, Seoul 08826, Republic of Korea

ARTICLE INFO

Keywords:
NaI(Tl)
Organic scintillator
Dark matter
Phoswich

ABSTRACT

Scintillating NaI(Tl) crystals are used for various rare decay experiments, such as dark matter searches. However, the hygroscopicity of NaI(Tl) crystals makes the construction of crystal detectors in these experiments challenging. Therefore, the crystal requires a tight encapsulation to prevent from air contact. More importantly, in a low radioactivity measurement, identification of external radiations and surface contamination is crucial to characterize the origin of total crystal radioactivities. Studies for the NaI(Tl) crystal encapsulation with active organic scintillator vetoes have been performed to mitigate the above-mentioned issues simultaneously. A bare crystal is directly coupled with liquid and plastic scintillators to tag external radiations that penetrate from the outer part of the crystal. We report the pulse shape discrimination between organic scintillator and the crystal scintillator in a single detector setup and their long-term stability.

1. Introduction

Since the first development of a thallium-doped sodium-iodide crystal, or NaI(Tl), for radiation detection [1,2], the scintillator has been employed across a wide range of applications from environmental monitoring to rare nuclear event searches. In particular, its high light yield [3] and wide dynamic range make it more attractive than any other scintillators. More recently, an improved light yield has made the crystals usable for low-energy dark matter search experiments [4].

Astrophysical observations infer that 27% of the universe is made of dark matter [5]. The dark matter is assumed to be composed of yet undiscovered particles of which Weakly Interacting Massive Particles (WIMPs) with masses between 1 and 100 GeV/c^2 and cross sections between 10^{-41} and 10^{-51} cm^2 are one of the leading candidates. WIMPs can elastically and coherently scatter off of the atomic nucleus. The nuclear recoil deposits its energy to the lattice structure of the target material in the range of 1 to 100 keV (electron-equivalent visible energy) [6]. The NaI(Tl) crystals show different amplitude-time responses depending on the type of radioactivities that can be used to discriminate a WIMP-induced signal from other ambient background radiations. For example, the decay time of an alpha-induced scintillation is 50 ns shorter than those of gamma or beta-induced scintillations that show a typical decay time of 250 ns.

NaI(Tl)-based experiments look for an isolated scintillation light induced by a nuclear recoil in an energy spectrum when a WIMP interacts in an array of the crystal detectors [7]. Typically, an array of segmented detector modules are used because the production of a high-quality, large volume crystal is technically challenging. Those modules are individually encapsulated under low humidity N_2 gas environment to protect a crystal from direct contact with air because the NaI(Tl) crystal can degrade its emission quality in the humid environment.

These crystal signals are read out by photomultiplier tubes (PMTs) which are attached via a thin light coupling interface. Because PMTs contain materials that have a relatively high radioactivity, these external gamma or beta radiations from PMT sneaking into the crystal are a significant background to the WIMP search especially in the lower end of the energy spectrum where a large amount of the WIMP signal is expected. Moreover, even after the careful encapsulation and shields, those dark matter experiments find a significant remnant ^{210}Pb contamination due to ^{222}Rn or other radioactive impurities [8–12] that are attached in the surface of the crystals mimicking WIMP-induced signals. Alpha particle decays in the bulk of the crystal would be easily identified by using a pulse shape discrimination(PSD) method [13], but those from the surface could be misclassified as a WIMP-nucleon interaction due to the relatively small deposited energy of a daughter isotope or the alpha particle itself [14].

Therefore, it is important to reduce the external background radiations using a veto detector and reject those surface alpha background events using a concept of a phoswich detector where two scintillators

* Corresponding author.
E-mail address: changhyon.ha@gmail.com (C. Ha).

https://doi.org/10.1016/j.nima.2019.163141
Received 13 August 2019; Received in revised form 15 November 2019; Accepted 17 November 2019
Available online 20 November 2019
0168-9002/© 2019 Elsevier B.V. All rights reserved.

with different decay times are coupled and read out together [15]. For instance, the Cryogenic Rare Event Search with Superconducting Thermometers (CRESST-II) experiment introduced a scintillating housing to achieve these two goals together, and they successfully shifted those background events away from the region of interest [16].

This paper reports an initial direct encapsulation of a bare NaI(Tl) crystal using an organic scintillator as an active veto which has been developed to solve the hygroscopic issue, to veto external radiations and to identify the surface radioactive contamination together.

2. Experimental setup

2.1. NaI(Tl) crystal encapsulation with liquid scintillator

Fig. 1(left) shows the experimental setup where a bare NaI(Tl) crystal is submerged in a liquid scintillator (LS) filled container. The crystal is positioned in the center of the container in direct contact with LS, and stabilized with a small acrylic structure. The cylindrical Teflon container is 50 mm-thick with 80 mm (diameter) and 80 mm (length). It also works as a diffusive light reflector. Two quartz glasses with stainless steel covers are used to light-couple and to seal the detector.

Properties of the LS have been widely studied in many experiments making a large volume and/or irregular shape of a detector possible. Among a wide range of solvents, we select linear alkyl-benzene (LAB), which has become increasingly popular thanks to its low toxicity and relatively low cost. This LAB-LS includes a few percents of 2,5-diphenyloxazole dissolved in the solvent for fluorescence and a trace amount of 1,4-bis[2- methylstyryl]benzene (bis-MSB) to improve the light properties [17]. The LAB-LS production is performed under controlled environment by supplying high-grade N_2 gas to prevent light output degradation caused by oxygen quenching [18].

The NaI(Tl) crystal is procured from Alpha Spectra Inc., who provided similar quality crystals of the COSINE-100 experiment [19]. Typical low-radioactivity crystals from the company exhibit light output of 15 photoelectrons per keV. Other properties of this scintillator are summarized elsewhere [19–21]. The particular crystal used here is rectangular in shape with a dimension of 25 mm × 24 mm × 38 mm.

The NaI–LS detector is coupled to the 3-inch PMTs made by Hamamatsu (R12669SEL) on each side, and then it is installed inside the low-background shield of the Korea Invisible Mass Search (KIMS) experiment facility in the 700-m-deep underground at the Yangyang Pumped Storage Power Plant [22]. An air-conditioner maintained (23.0 ± 0.1) °C inside the shields throughout this measurement. Signals from both PMTs are amplified by a factor of 30, and a 400 MSPS[1] fast analog-to-digital converter(FADC) was used as a digitizer. PMT summed signals are used to make the energy spectrum calibrated with a disk-shaped ^{60}Co gamma source (~1 μCi) that emits 1173 and 1332 keV gamma-rays and 60 keV ^{241}Am gammas. Also, background-only underground data are used to analyze the detector performance.

2.2. NaI(Tl) crystal encapsulation with a plastic scintillator

In this setup, the plastic scintillator (PS) is used as a veto detector as well as an encapsulation material. A bare cubic NaI(Tl) crystal is submerged in the partially polymerized scintillating resin[2] which is slowly hardened as a plastic scintillator to encase the bare crystal as shown in Fig. 1(right). We perform the hardening process as instructed in the manual but it is challenging for an NaI(Tl) encapsulation due to its chemical reaction with the crystal. Even if this casting procedure is carried in a low-humidity metallic glove box, depending on the ambient temperature and related hardening speed, the resulting products show degradations on the surface either by a changed color or by forming bubbles. One of these NaI–PS casting products is machined into a cylindrical shape with 50 mm diameter and 40 mm length, and then is polished to make the surface of the plastic scintillator transparent. The cylinder is wrapped with several soft Teflon layers for light reflection and one end of the cylinder is light-coupled with a 2-inch Hamamatsu PMT (H7195) using silicone grease. We use a 500 MSPS FADC digitizer with an improved timing resolution and dynamic range. This measurement is carried out in a ground-floor laboratory with ^{241}Am and ^{60}Co radioactive sources. Due to high background radiations in the ground laboratory, we could not measure a long-term background-only data.

[1] Megasamples per second.

[2] The product EJ-290 from Eljen Inc. is used.

3. Methods

3.1. Pulse shape discrimination

The pulse shape of the output signal from a scintillator can be used to identify different radioactive isotope types, since the interaction of a heavier particle can cause transitions to more complex molecular or lattice energy states resulting in different amplitude-time response [23, 24]. Therefore, typical observables take advantage of the pulse's decay time.

Similarly, in these hybrid scintillator setups, we differentiate NaI(Tl)-induced signals from organic scintillator-induced signals using their intrinsic decay times. The decay time of a NaI(Tl) crystal is around 250 ns, whereas that of an organic scintillator is less than 10 ns [25].

Here, we use the discrimination observable "Mean time" [26], or amplitude-weighted average time of a pulse, defined as

$$\text{Mean time } (\mu s) = \frac{\sum_i^{bins} q_i t_i}{\sum_i^{bins} q_i}, \quad (1)$$

where q_i and t_i are ith bin amplitude and its time respectively. *Bins* run for 1000 ns from the trigger position. Though the Mean time is strongly correlated with the pulse's decay time, it presents slightly shorter time than the decay time depending on how many bins are integrated. Since it only takes into account characters of the waveform shape, its minimal energy dependence helps reduce the bias due to event selection.

3.2. The measurements made and various sources

With the PSD method, we characterize three different cases of measurements: NaI-PS with a single PMT, NaI-LS with two PMTs, and the same NaI-LS setup in a freezer. Using ^{241}Am and ^{60}Co gamma sources, only the NaI crystal's energy scales and resolutions in keV are determined and the veto scintillator's energy scale is not separately adjusted when plotting the energy as a function of the Mean time. Light yields of those three cases are measured using single photoelectron spectrum with isolated single photons after a few μs starting from the leading edge of the 60 keV ^{241}Am gamma signal waveforms. We have also tested the consistency of the energy spectrum and light yields using the known internal gamma lines present in the crystal bulk.

4. Results

4.1. Signal shape of crystal scintillator versus organic scintillator

The plastic scintillator used in this experiment is known to have a short decay time around ~ 3 ns [27]. Thus, the maximum signal height from the plastic scintillator shows a relatively higher value than that from the NaI(Tl) crystal scintillator for the same deposited energy. Therefore, a wide dynamic range of DAQ is required to measure plastic and NaI(Tl) signals simultaneously. Fig. 2(a) shows the Mean time distribution as a function of an electron-equivalent energy for the 60 keV ^{241}Am gammas at the energies between 0 and 120 keV. The Mean time variable can separate different scintillation signals among the plastic scintillator, crystal scintillator, or both scintillators together. Fig. 3(a) shows a high-energy distribution of NaI–PS up to 2000 keV when measured with a ^{60}Co gamma source. Two prominent bands at

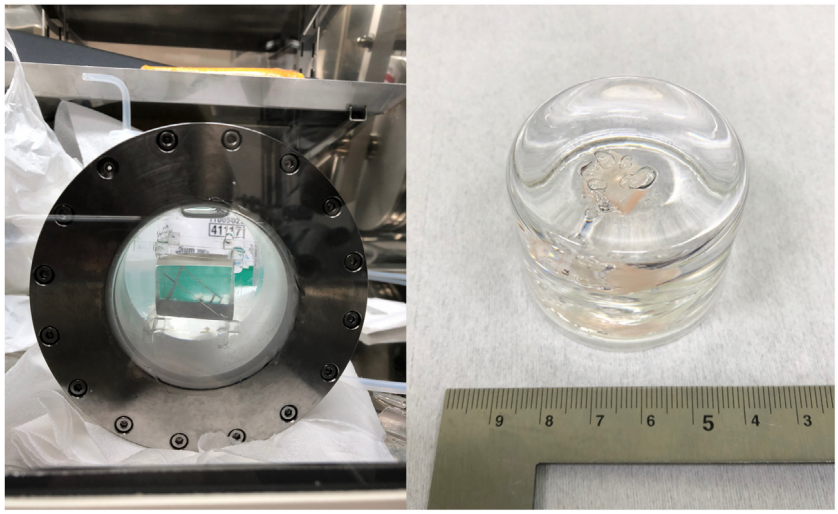

Fig. 1. NaI(Tl) crystals encased with liquid scintillator (left), and plastic scintillator (right). In the NaI–LS setup, the crystal is centered by using a small acrylic structure which shows a similar index of refraction as the liquid scintillator. For the NaI–PS setup, a crystal was encased by placing at the center of the half-hardened plastic resin and filling the rest of the resin to seal completely.

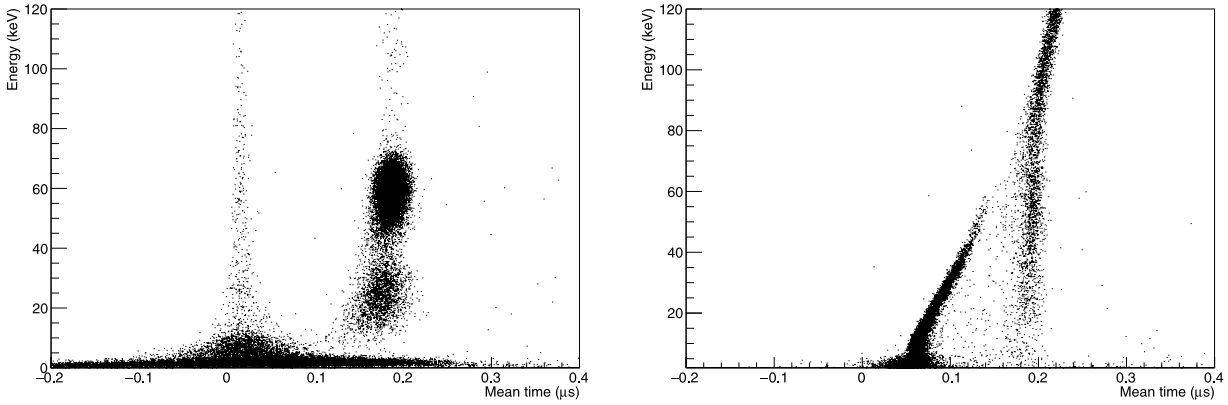

Fig. 2. Mean weighted time distribution of crystal-plastic detector (a) as well as crystal-liquid detector (b). Plastic scintillator signal and crystal signal are well separated. Liquid scintillator signal is also well separated from crystal signal but two signals merge at around 60 keV region due to a shorter dynamic range of our DAQ that makes top of the LS waveforms artificially cut away at the time of measurements. The energy range between 0 and 120 keV is chosen by DAQ dynamic range focusing on the region of interest below 20 keV.

approximately 20 ns and 200 ns are shown for plastic signals and crystal signals, respectively. Events between those two bands contain merged scintillation signals.

A good separation is also seen with background-only data in the NaI–LS setup as shown in Fig. 2(b) for low-energy up to 120 keV and in Fig. 3(b) for high-energy up to 3500 keV. Because the NaI–LS measurement is performed using background-only data, internal alpha particle events around 3000 keV (5400 keV deposit energy for the ^{210}Po alpha decay) with a 50 ns shorter Mean time is also shown compared with the gamma bands. However, in this setup, due to hardware limitation, the LS signal band at around 50 ns is tilting towards the beta and gamma band between 10 and 60 keV region. This is because the relatively tall LS signal is saturated faster than that of crystal signal waveforms.

Both setups show a good separation between organic scintillation and inorganic scintillation. The crystal produces more light from deposited energy than does the plastic scintillator due to their different quenching factors [28]. Additionally, a full peak of the source is seen in the crystal while that is not well observed in the plastic or liquid due to their different range characteristics.

Fig. 4 shows the energy spectra for each band in the NaI-PS setup after selecting events within 3σ from the mean of each band. The energy spectra of the crystal is calibrated using the known peaks of ^{60}Co, whereas the plastic is calibrated by using the Compton edge.

4.2. Merged signal identification

Merged signals can occur when a particle interacts with both the crystal and the plastic or liquid. This signal can be caused by Compton scatterings or a surface alpha decay process near the surface of the NaI(Tl) crystal, as shown in Fig. 5. These merged signal waveforms (Fig. 5(b) and (c)) contain both the short decay and long decay components. They were selected in the same energy range (200–400 keV) and increasing Mean time from Fig. 3 (a) to show the relative signal height and shape depending on the fraction of a different waveform mixing.

4.3. Low temperature measurements of NaI–LS

For both NaI–LS and NaI–PS tests, their light yields show decreasing behavior during the measurements. We suspect that remnant moisture, moisture diffusion, or unknown chemical reactions would affect the NaI(Tl) surface quality which influences on the measured light yield.

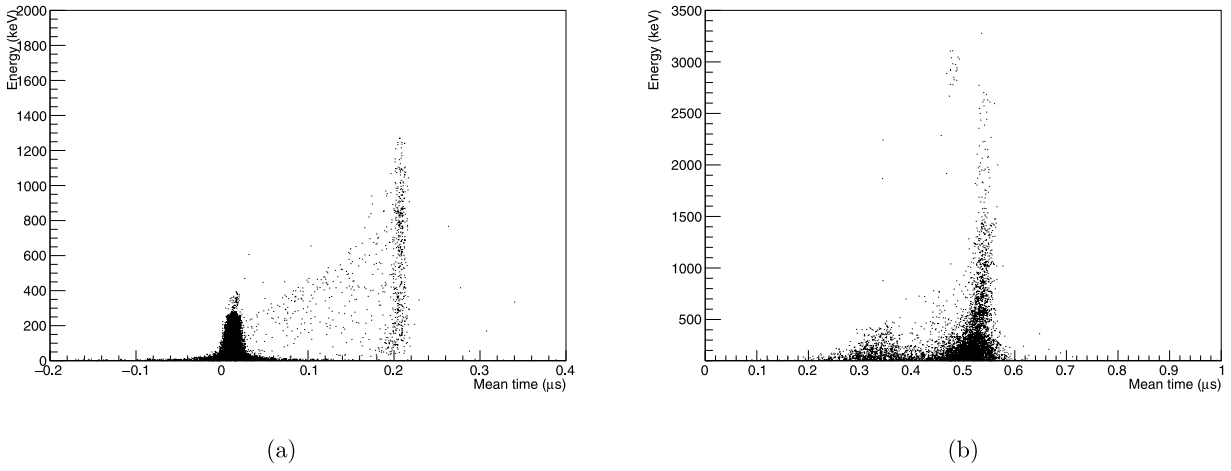

Fig. 3. Mean weighted time distribution of both setups emphasizing on the high energy part of DAQ. The 5th dynode of the PMTs are read out to extend the dynamic range at a cost of the low-energy resolution. NaI–PS measurements (a) are done with ^{60}Co radioactive source while the NaI–LS data (b) show background-only run. Both show again a good pulse shape separation between organics and inorganics. In the NaI–PS (a) plot between two bands, event populations which contain both signals from plastic and crystal. Because in the plastic scintillator the light loss is more severe than in the crystal, the merged signal energy is increasing as a function of increasing mean time. Below 500 keV region, the NaI–LS data show a similar behavior. Also, at higher energies around 3000 keV, PSD between crystal alpha, and crystal beta and gamma is retained.

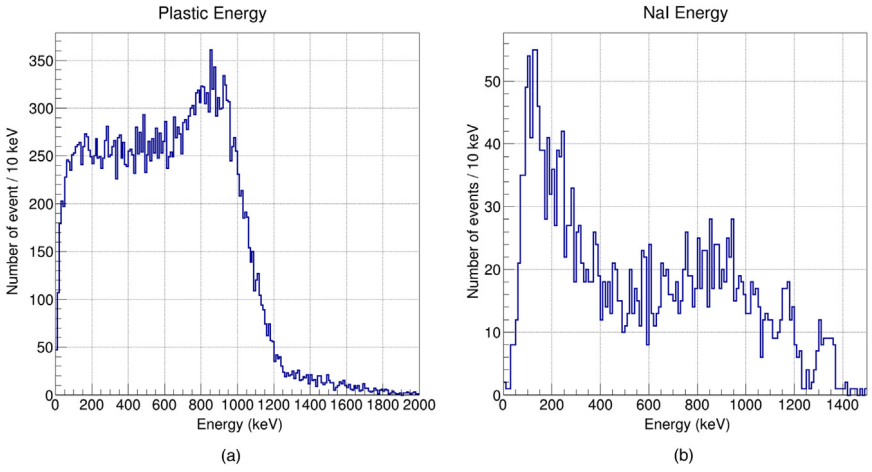

Fig. 4. Plastic (a) and crystal (b) scintillator energy spectra. A Compton edge fitting is used to calibrate the energy spectra of plastic scintillator, whereas the full peaks are used for crystal.

To eliminate the moisture attack in the setup, the NaI–LS detector is put in the freezer.

We use a commercial freezer which keeps temperature at −35 °C. The calibration factor and the light yield are regularly measured at the Kyungpook National University laboratory using 60 keV ^{241}Am gamma source with which we find NaI(Tl) exhibits the light yield of 11.3 ± 1.0 ph/keV. Considering light yield variation [29], systematic uncertainties, and PMT effects, this result is comparable with those for other crystals from the same company. The light yield of NaI–LS detector at the room temperature is decreasing over time, whereas the light yield is stable at the low temperature environment for 121 days (see Fig. 6).

5. Conclusion

NaI(Tl) crystal has been encapsulated by organic scintillators to prevent humidity and to tag external radiation. LAB-based liquid and plastic scintillator are used to encompass the crystal with direct optical contact. Light yields of NaI(Tl) are measured to be (11.3 ± 1.0) and (1.2 ± 0.2) pe/keV for liquid and plastic scintillator encapsulation, respectively. A PSD analysis confirms that organic and inorganic scintillator light signals are relatively well separated. (more than 5 σ at 400 keV). Furthermore, waveform signals resulting from simultaneous energy deposition in both scintillators are identified. In the long-term measurements, NaI-PS is chemically unstable while NaI-LS shows degradation in light quality possibly due to humidity diffusion to the crystal. We have also investigated long-term light yield stability at low temperature (−35 °C) for liquid scintillator encapsulation. This study shows that a stable light yield has been achieved over four months, since humidity effects on the crystal surface might have been reduced below freezing temperature. In contrast, ambient temperature measurements show approximately 30% light yield reduction over one month. In the future, we plan to study the surface ^{210}Pb(^{210}Po) contamination occurring near the boundary or at the surface between a crystal and an organic scintillator, which could be identifiable by tagging ^{210}Po alpha particles in an organic scintillator and measuring nuclear recoil (^{206}Pb) in the crystal with the similar setup as discussed in the current paper.

Declaration of competing interest

The authors declare that they have no known competing financial interests or personal relationships that could have appeared to influence the work reported in this paper.

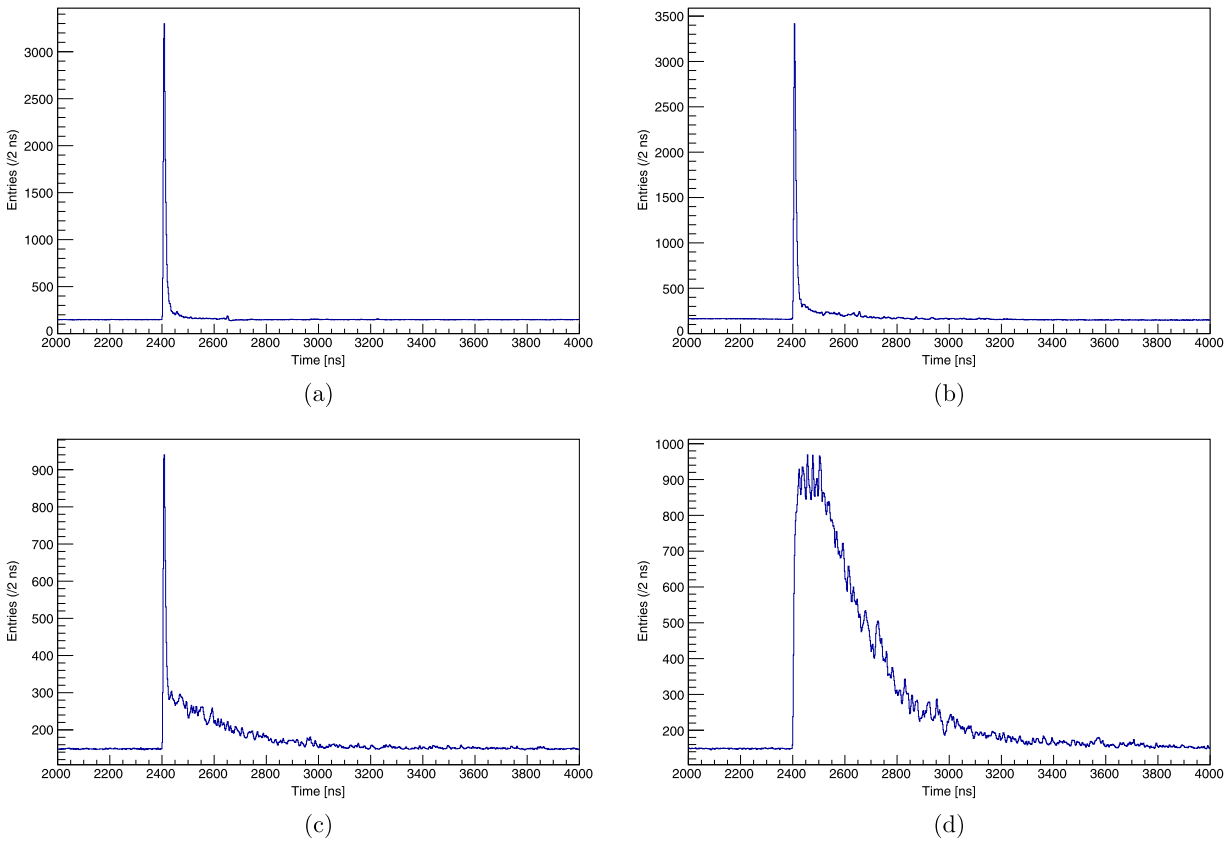

Fig. 5. Raw waveforms depending on the signal types obtained from Fig. 3 (a). To compare the relative heights and shape of the merged signals, we sample events from the 200–400 keV band in energy with increasing the Mean time values. (a) and (d) figures are from plastic and crystal events, respectively, whereas (b) and (c) show mixed signals from both scintillators.

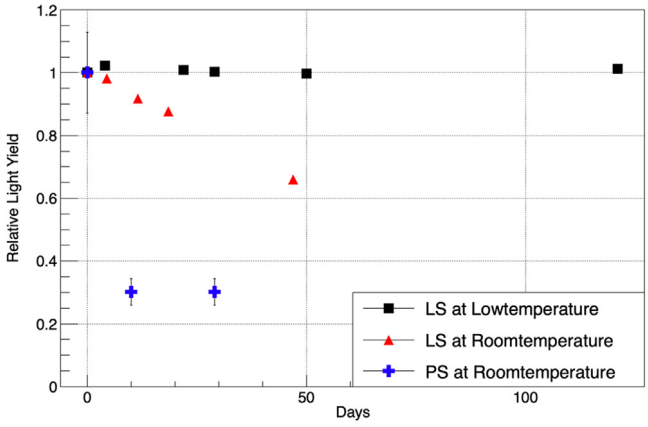

Fig. 6. Single photoelectron relative light yields as a function of time for several conditions. The light outputs both for NaI-PS at room temperature (blue cross) nd NaI-LS at room temperature (red triangle) show decreasing behavior over time while that of NaI-LS at low temperature (black square) shows stable condition.

Acknowledgments

This research was funded by the Institute for Basic Science (Korea) under project code IBS-R016-A1; NRF (National Research Foundation of Korea) Grant funded by the Korean Government (NRF-2016-Fostering Core Leaders of the Future Basic Science Program/Global Ph.D. Fellowship Program.); National Research Foundation of Korea (NRF) funded by the Ministry of Science and Technology, Korea (MEST, No. 2018R1A6A1A06024970).

References

[1] R. Hofstadter, Phys. Rev. 74 (1948) 100.
[2] R. Hofstadter, Phys. Rev. 75 (1949) 796.
[3] I. Holl, E. Lorenz, G. Mageras, IEEE Trans. Nucl. Sci. 35 (1988) 105.
[4] N.J.C. Spooner, et al., Phys. Lett. B 321 (1994) 156.
[5] P.A.R. Ade, et al., Astron. Astrophys. 594 (2016) A13.
[6] Marc Schumann, J. Phys. G 46 (2019) 103003.
[7] R. Bernabei, et al., Phys. Lett. B 389 (1996) 4.
[8] S. Cebrián, et al., Nucl. Phys. B (Proc. Suppl.) 114 (2003) 111.
[9] G. Adhikari, et al., Eur. Phys. J. C 77 (2017) 437.
[10] The EDELWEISS Collaboration, Astropart. Phys. 28 (2007) 1.
[11] R. Agnese, et al., Phys. Rev. Lett. 112 (2014) 241302.
[12] D.S. Akerib, et al., Phys. Rev. Lett. 112 (2014) 091303.
[13] K.W. Kim, et al., Astropart. Phys. 62 (2015).
[14] K.W. Kim, et al., Astropart. Phys. 102 (2018).
[15] Travis L. White, William H. Miller, Nucl. Instrum. Methods A 422 (1999).
[16] R. Stauss, et al., Eur. Phys. J. C 75 (2015) 352.
[17] J.S. Park, et al., Nucl. Instrum. Methods A 851 (2017).
[18] Ba Ro Kim, et al., J. Radioanal. Nucl. Chem. 310 (2016) 1.
[19] G. Adhikari, et al., Eur. Phys. J. C 78 (2018) 107.
[20] P. Adhikari, et al., Eur. Phys. J. C 76 (2016) 185.
[21] G. Adhikari, et al., Eur. Phys. J. C 77 (2017) 437.
[22] H.S. Lee, et al., Nucl. Instrum. Methods A 571 (2007) 3.
[23] R. Bernabei, et al., Nuovo Cimento A 112 (1999) 6.
[24] Gioacchino Rauncci, Augusto Goretti, Paolo Lombardi, Nucl. Instrum. Methods A 412 (1998) 2–3.
[25] G.F. Knoll, Radiation Detection and Measurement, fourth ed., John Wiley & Sons, Inc, 2010.
[26] H.S. Lee, et al., Phys. Rev. Lett. 108 (2012) 181301.
[27] https://eljentechnology.com/products/plastic-scintillators/ej-290.
[28] H.W. Joo, et al., Astropart. Phys. 108 (2019) 50.
[29] M. Moszyński, et al., Nucl. Instrum. Methods A 568 (2006).